# Resonators of IR lasers based on two-dimensional photonic crystals for organization of surface output of radiation

© I.V. Oreshko, V.V. Zolotarev , S.O. Slipchenko, A.E. Kazakova, N.A. Pikhtin

loffe Institute,

194021 St. Petersburg, Russia

¶ E-mail: zolotarev.bazil@mail.ioffe.ru

Received March 6, 2025 Revised April 25, 2025 Accepted May 7, 2025

Within the AlGaAs/GaAs/InGaAs heterostructure, the output losses were calculated for resonators based on 2D photonic crystals with square symmetry lattice, which nodes formed in the upper cladding layer of the laser waveguide by holes of different symmetries. It is shown theoretically that, in contrast to photonic crystals formed by holes with  $C_2$  symmetry, characterized by the presence of high-Q modes with zero output losses, photonic crystals formed by holes in the shape of isosceles right triangles or equilateral trapezoids demonstrated the greatest mode discrimination between the two lowest-threshold modes with non-zero output losses. Calculations of output losses show that the most preferable designs with holes characterized by a large depth, leaving a thin  $(\sum 0.1 \text{ microns})$  residual layer between the photonic crystal region and the waveguide, and the final optimization of the output loss value should be performed with a known value of internal optical losses in a specific heterostructure.

Keywords: semiconductor lasers, photonic crystal, distributed feedback, cavity modes.

DOI: 10.61011/SC.2025.02.61369.7665

### 1. Introduction

Semiconductor lasers emitting from the surface of a chip with a resonator based on a two-dimensional (2D) photonic crystal (PC) are of considerable interest for modern photonics and optoelectronics, since they allow obtaining an output laser beam of large area and small symmetrical divergence [1-6] directed along the normal to the heterostructure surface. A symmetrical radiation pattern with a small divergence angle makes it possible to significantly increase the efficiency of laser radiation input into optical fibers or to form new areas of direct application of high-power semiconductor lasers. Modern LiDAR (Light Detection and Ranging) systems used in unmanned vehicle control may be one of the most sought-after applications for such lasers. The 2D-PC band structure also forms spectral selection, which makes it possible to obtain single-mode coherent radiation [7,8] with a narrow spectrum, which is in great demand in optical communication systems in free space. The geometric parameters of the PC (the shape and dimensions of the air holes forming the PC; the size of the radiation aperture) determine, among other things, the optical output losses (Q factor of the resonator), the polarization and the radiation pattern of the outgoing beam [9–11].

The great potential of surface-studying lasers based on 2D photonic crystals requires the development of models in order to optimize the design parameters of the resonator and photonic crystals for various applications. These calculation models should demonstrate the relationship between the design parameters of photonic crystals, such as the geometric shape and symmetry of the holes, with the characteristics of the resonator and its radiative efficiency.

The Finite-Difference Time-Domain (FDTD) [12–14] and the Three-Dimensional Finite Element Method (3D FEM) are among the most popular methods for calculating such complex structures as PC [15–17]. However, both methods have a number of disadvantages related to the requirement of significant computing power, especially for calculating large-area structures (on the order of hundreds of lattice periods of PC), which are commonly used in real surface-emitting lasers.

Therefore, a number of semi-analytical methods for calculating the characteristics of a resonator formed by PC were previously developed based on the Coupled Wave Theory (CWT) [18,19]. The Sakai's initial two-dimensional calculations [20,21] assumed that the field distribution along the axis of growth of the heterostructure is a plane wave, which does not reflect the actual waveguide properties of the laser heterostructure. A solution to this problem was proposed in Ref. [22] based on the Strafer technique [19] for lasers with one-dimensional distributed feedback (DFB). The essence of the method consists in separating variables and decomposing the electromagnetic field according to Bloch's theorem, thus, the resulting fields are represented as the product of the fundamental mode of a multilayer waveguide heterostructure, depending only on z-coordinates and related PC modes, depending on x-, y-coordinates.

In this paper, we consider a model of an infinite 2D-PC with square symmetry and transverse electric polarization as part of a four-layer waveguide laser structure. We performed the calculations specifically for an infinite crystal, since real surface-emitting lasers use structures of the order of hundreds of periods of the PC lattice, which is necessary to increase the optical output power. The study of infinite PC allows obtaining fundamental patterns between the

PC parameters and the characteristics of a semiconductor laser resonator. This approximation makes it possible to significantly simplify calculations by eliminating boundary conditions and reducing the system of differential equations to a system of ordinary linear equations.

The 3D-CWT method developed in Ref. [22] was used for calculating photonic crystals. This method allows calculating the photonic crystals of square symmetry with an arbitrary shape of the holes. The condition for the applicability of this method is a small coupling coefficient ( $\kappa\Lambda \ll 1$ , where  $\kappa$  is the coupling coefficient,  $\Lambda$  is the period of the photonic crystal), in which the period of energy exchange of two coupled waves is much longer than the period of the photonic crystal, which corresponds to our case. Unlike the authors of Ref. [22], we introduce a significant structural difference, assuming that the PC is surface (unprotected), i.e., a layer with periodic changes in dielectric constant is formed in the upper plate of the laser waveguide (p-emitter). This choice of design is attributable to the greater simplicity of the technological implementation of the calculated structure, since it eliminates two-stage epitaxial growth. This study focuses on the analysis of output losses as a critically important parameter that is used to optimize the power and threshold characteristics of semiconductor lasers, as well as form the requirements for the core design (material gain, optical limitation factor). The results were obtained for PC with different shapes of air holes with different symmetries (circle, triangle, rectangle, trapezoid). Optical output losses and wavelengths for various modes were calculated for all types of holes, and losses were analyzed depending on the depth of etching of the holes.

### 2. Calculation method

### 2.1. General provisions

One of the most important features of surface-emitting lasers based on two-dimensional photonic crystals is the possibility of strictly vertical laser beam output. This advantage is realized by meeting the conditions of the 2nd order Bragg diffraction. For wavelengths corresponding to the Bragg condition,  $\lambda = 2n_{\rm eff}\Lambda/N$ , where  $\lambda$  is the wavelength emitted by the laser,  $n_{\rm eff}$  is the effective refractive index of the heterostructure waveguide mode, and N=2 is the diffraction order; distributed feedback is formed in the plane of the waveguide layer, which determines the resonator properties of the PC and diffracted laser radiation propagating orthogonally to the crystal plane (optical output power).

In our paper, we consider 2D-PC with simple square symmetry. Structurally, it consists of air holes etched into the material of the *p*-emitter of the laser heterostructure (Figure 1). Thus, the difference between the dielectric permittivity of the emitter  $\varepsilon_b$  and the air  $\varepsilon_a$  creates a two-dimensional photonic crystal lattice, which is characterized by an average dielectric constant  $\varepsilon_{av} = f\varepsilon_a + (1-f)\varepsilon_b$ ,

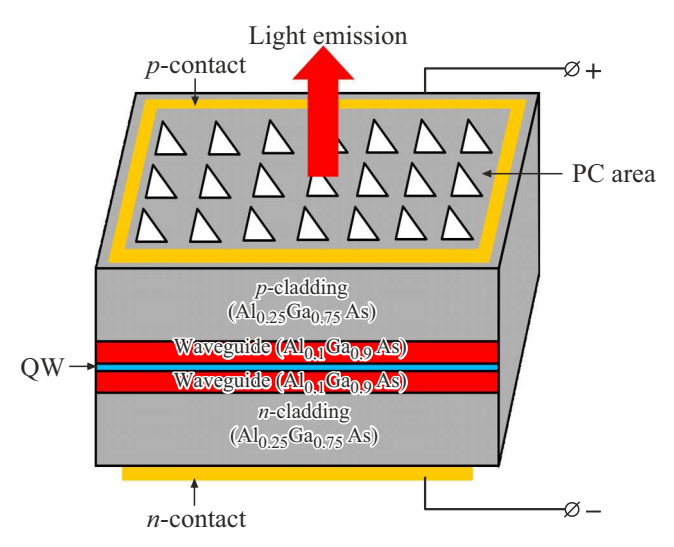


**Figure 1.** Schematic representation of a laser structure with a PC region formed on the surface of the *p*-emitter.

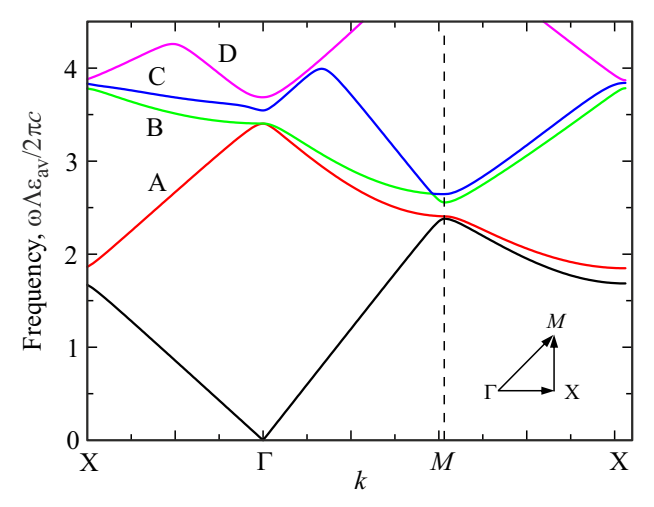


**Figure 2.** Photonic band structure of a square-symmetrical PC formed by holes shaped like an isosceles right triangle.

where f — fill factor, a dimensionless parameter determined by the ratio  $f = S_{\text{hole}}/S_{\text{cell}}$ , in which  $S_{\text{hole}}$  is the area of the air hole, depending on its geometry, and  $S_{\text{cell}} = \Lambda^2$  — PC lattice cell area.

The 2D-PC square lattice has a characteristic band structure with three extreme points —  $\Gamma$ , X, and M (Figure 2) attributable to its symmetry [23,24].  $\Gamma$ -point of the 2nd order in the center of the Brillouin zone corresponds to the Bragg condition with N=2 in which distributed feedback and radiation diffraction occur in the direction normal to the surface of the structure. In the general case, we observe 4 dispersion frequency branches corresponding to 4 modes — A, B, C, and D for the considered PC symmetry at the point  $\Gamma$  for the field polarization. The emissivity of these modes is characterized by optical output losses, which in turn depend on the parameters of the

geometric shape and symmetry of the air hole, as well as its size. One of the main goals of our calculation is to analyze the effect of these factors on the emissivity of PC and determine which of the modes will emit most effectively.

#### 2.2. Formulation of the model

This paper is focused on the consideration of the TE-polarization of the field, the electric field is distributed strictly in the PC plane. This choice is attributable to the active region, which for near-IR lasers (950–1100 nm) is most often formed by an elastically stressed InGaAs quantum well, for which stimulated recombination is characterized by TE polarization.

The fundamental method of our calculation is the idea, standard for periodic structures, of decomposing the electric field inside the PC into individual harmonics in accordance with the Bloch theorem [25], according to which the amplitude of the field inside a structure with translational symmetry should have the same periodicity:

$$E_i(\overrightarrow{r}) = \sum_{m,n} E_{i,m,n}(z) \cdot e^{-i(m\beta_0 x + n\beta_0 y)}, \quad i = x, y, \quad (1)$$

where  $E_{i,m,n}$  is the distribution of the electromagnetic field along the axis of growth of the heterostructure, waveguide mode;  $\beta_0 = 2\pi/\Lambda$  is the component of the reciprocal lattice vector PC, m and n are arbitrary integers. Due to the fact that PC is a periodic structure, the refractive index in the PC layer can also be represented as a Fourier series:

$$n^{2}(x, y) = n_{0}^{2} + \sum_{m \neq 0, n \neq 0} \xi_{m,n} \cdot e^{-i(m\beta_{0}x + n\beta_{0}x)}, \qquad (2)$$

where  $n_0^2 = \varepsilon_{av}$  is the average dielectric constant PC,  $\xi_{m,n}$ —are the amplitudes of the Fourier expansion. This expression is executed only in the PC layer. The amplitudes of the Fourier decomposition are zero outside the region of the photonic crystal; inside the PC, the amplitudes of the Fourier decomposition are determined by the integral relation:

$$\xi_{m,n} = (1/\Lambda^2) \cdot \iint_{PC} \Delta n^2 \cdot e^{i(m\beta_0 x + n\beta_0 y)} dx dy, \qquad (3)$$

where  $\Delta n^2 = \varepsilon_a - \varepsilon_b$  is the difference of PC dielectric permittivities. The integration is carried out over a primitive cell (coinciding with the Wigner-Seitz cell) and the integral is normalized to its area —  $\Lambda^2$ . PC is the area corresponding to the geometric shape of the hole of the photonic crystal. Thus, the limits of the double integral depend on the geometry and symmetry of the air opening and affect such characteristics of the PC-based resonator as optical output losses and resonant wavelength.

The solution of Maxwell's equations and the transition to a system of coupled mode equations are presented in detail in Ref. [22], so we will not repeat it here, but we will note a number of characteristic results. The decomposition of the electromagnetic field in expression (1) is divided into groups depending on the magnitude of the wavenumber in the PC plane: basic waves —  $\sqrt{(m^2+n^2)}=1$ , high-order waves —  $\sqrt{(m^2+n^2)}>1$  and radiative waves —  $\sqrt{(m^2+n^2)}=0$ . The basic waves are waves corresponding to the four propagation directions +/-x and +/-y, for which the distribution of electromagnetic radiation along the axis of growth of the heterostructure corresponds to the fundamental waveguide mode calculated from the approximation of the absence of PC (PC is replaced by a continuous layer with  $\varepsilon=\varepsilon_{av}$ ):

$$E_{y,1,0} = \Theta(z) \cdot R_x, \quad E_{y,-1,0} = \Theta(z) \cdot S_x,$$
  
 $E_{x,0,1} = \Theta(z) \cdot R_y, \quad E_{x,0,-1} = \Theta(z) \cdot S_y.$  (4)

An emissive wave with a wave vector in the PC plane equal to zero  $(k_{x,y} = 0)$  generates output radiation from the crystal surface. For the case of infinite PC, the values  $(R_x, S_x, R_y, S_y)$  are not functions of coordinates (x, y), which allows the system of differential equations of coupled modes to be transformed into a system linear equations with respect to the amplitudes of the base waves:

$$\varphi_q V = C_{\text{sum}} V, \tag{5}$$

where  $\phi_q$  is the eigenvalues of the matrix  $C_{\text{sum}}$ ,  $\mathbf{V} = (R_x, S_x, R_y, S_y)^t$  is the mbox4-dimensional vector whose components are the amplitudes of the base waves,  $C_{\text{sum}} = C_{180^{\circ}} + C_{\text{rad}} + C_{\text{highorder}} - \text{matrix } 4 \times 4 \text{ of integral}$ coupling coefficients. The form of the matrices  $C_{180^{\circ}}$ ,  $C_{\text{rad}}$ ,  $C_{\text{highorder}}$  is also described in detail in Ref. [22]. C180° matrix expresses a one-dimensional relationship between two waves propagating in the PC plane (for example,  $R_x$ ,  $S_x$ ), its elements are similar to the coupling coefficients for a one-dimensional optical laser obtained in Ref. [19]. The matrix  $C_{\rm rad}$  consists of coefficients linking the base waves and the radiative wave. The matrix  $C_{highorder}$  characterizes the relationship of higher-order waves (with a wave vector in (1) with  $\sqrt{(m^2 + n^2)} > 1$ ). Generally speaking, in (1) the summation of m and n occurs from minus infinity to plus infinity, however, our preliminary calculations showed that as the harmonic number increases, its contribution to the solution is (5) it gets smaller and smaller, and the values of the eigenvalues of the matrix  $C_{\text{sum}}$  almost stop changing. In our calculation of the matrix  $C_{highorder}$ , summation took place for  $-10 \le m$ ,  $n \le 10$ , i.e.  $21 \times 21$  harmonics was used.

The complex-valued eigenvalues of the matrix  $C_{\rm sum}$ , with a dimension of cm<sup>-1</sup>, determine the optical output loss and deviation from the Bragg wavelength for each of the four modes at the  $\Gamma$ -point of the 2nd order (A, B, C, or D). The imaginary part of the eigenvalues corresponds to optical output losses (in the approximation of the absence of internal optical losses), the real part corresponds to the deviation of the wave vector of the mode from the Bragg wave vector, from which the wavelength of the mode can be determined from the ratio

$$\lambda_q = 2\pi n_{\text{eff}} / \left( \text{Re} \left( \varphi_q \right) + \beta_{\text{Bragg}} \right).$$
 (6)

Laser heterostructure parameters

Layer	Thickness, microns	Refractive index
<i>n</i> -Emitter	2	3.385
Waveguide	0.3	3.449
<i>p</i> -Emitter	2	3.385
PC area	1.9	$\sqrt{arepsilon_{av}}$

The eigenvector V contains the amplitudes of the base waves for each mode, and it can be used to find amplitudes of higher orders and, thus, construct the distribution of the electric field in the PC plane. Thus, the problem of finding fields inside a PC is reduced to the problem of eigenvalues and eigenvectors of the matrix operator  $C_{\text{sum}}$ .

### Description of the calculated laser structure

As a starting point for calculations, we use a classical laser heterostructure based on a symmetrical 3-layer optical waveguide with air holes etched in the upper emitter that form a PC (see Figure 1). A strained InGaAs quantum well has been formed in the center of the waveguide, which is a source of laser radiation generation with a wavelength of  $\sim 1.045$  microns. We assume that the size of the quantum well ( $\sim 8 \, \text{nm}$ ) is extremely small in comparison with the wavelength of the radiation, therefore, its refractive index cannot be taken into account when calculating the waveguide. The materials of the emitters and waveguide are a semiconductor solid solution  $Al_xGa_{1-x}As$ , in which the proportion of Al is 25% for the emitters and 10% for the waveguide. PC lattice period is chosen in such a way as to comply with the condition of the 2nd order Bragg diffraction, and is  $\sim 0.305$  microns.

The refractive indices of the emitters and waveguide were calculated using a simplified model of interband transitions for materials with a zinc blende type lattice [26]. The calculated refractive indices of the layers for the Bragg wavelength and layer thickness are shown in the table. The refractive index of the photonic crystal region corresponds to the average permittivity  $\varepsilon_{av}$ , which depends on the transverse dimensions of the air holes.

### 4. Simulation results and discussion

## 4.1. The effect of the shape of the air holes on the output loss at a fixed etching depth

The output losses determine the threshold conditions for mode generation and the efficiency of laser radiation. The generation threshold conditions are primarily met for the mode with minimal output losses, thus, one (or two, in the case of degeneracy) of the four modes has priority for generation. The greater the mode discrimination between the mode with the lowest output loss and the

second mode following it, the more stable the single-mode regime will be maintained over a larger range of pumping currents. If the output losses turn out to be zero, then the emission of such a mode into free space becomes impossible. This mode characterizes a resonator with a high quality factor (assuming low internal optical losses), but it does not allow achieving high optical output power. Each of the modes (A, B, C, D) is characterized by its own optical loss.

In addition to the symmetry of the lattice, losses also significantly depend on the shape and size of the air hole itself. Initially, we calculated and analyzed how the magnitude of output losses changes with a change in the lateral dimensions of the hole, with the etching depth fixed at 1.9 microns, i.e., the waveguide and the PC are separated by a residual layer of the p-emitter with a thickness of 0.1 microns. For the convenience of comparing dependencies corresponding to different types of geometries, loss graphs were constructed depending on the fill factor.

Figure 3, a shows the dependences of the output loss on the fill factor for the PC formed by round holes for four modes. A pairwise degeneracy of modes is observed owing to symmetry, modes C and D have the same losses and are radiative, the losses of modes A and B are not only equal, but are also equal to zero. The laser radiation will practically not leave the crystal during laser generation in a resonator of this design, since the threshold conditions of generation will be met primarily for modes A and B. Thus, PC with round holes is well suited for tasks that require a resonator with a high quality factor, and is not suitable for high-power injection lasers.

Degeneracy is eliminated for holes with the shape of an isosceles right triangle (Figure 3, b) and an equilateral triangle (Figure 3, c), and all modes have nonzero output losses at high values of the fill factor. The priority mode is mode B in case of a right-angled triangle (Figure 3, b), up to a fill factor of 25%, mode A becomes the priority mode with an increase in the fill factor. There will be a mode competition with the fill factor  $\sim 25\%$ , while the wavelength of the modes A and B does not match, there is no degeneracy, which will cause a multimode generation mode. Thus, this point is not suitable for a single-mode resonator for high-power semiconductor lasers. Mode B is the priority mode for an equilateral triangle (Figure 3, c) up to the maximum value of the fill factor of 40%. However, the mode discrimination in absolute value is less than for a right-angled triangle.

To determine the fundamental causes of the appearance of zero-loss modes, we performed calculations of PC with rectangular holes (Figure 3, d) and holes with two bends (in the shape of a rectangular letter Z) (Figure 3, e). These shapes are chosen based on considerations of symmetry. The rectangle has a symmetry of  $C_2$  and a specular reflection. Two modes with zero output losses are also observed for this design. To separate  $C_2$ -symmetry and specular reflection, calculations were performed for Z-shape

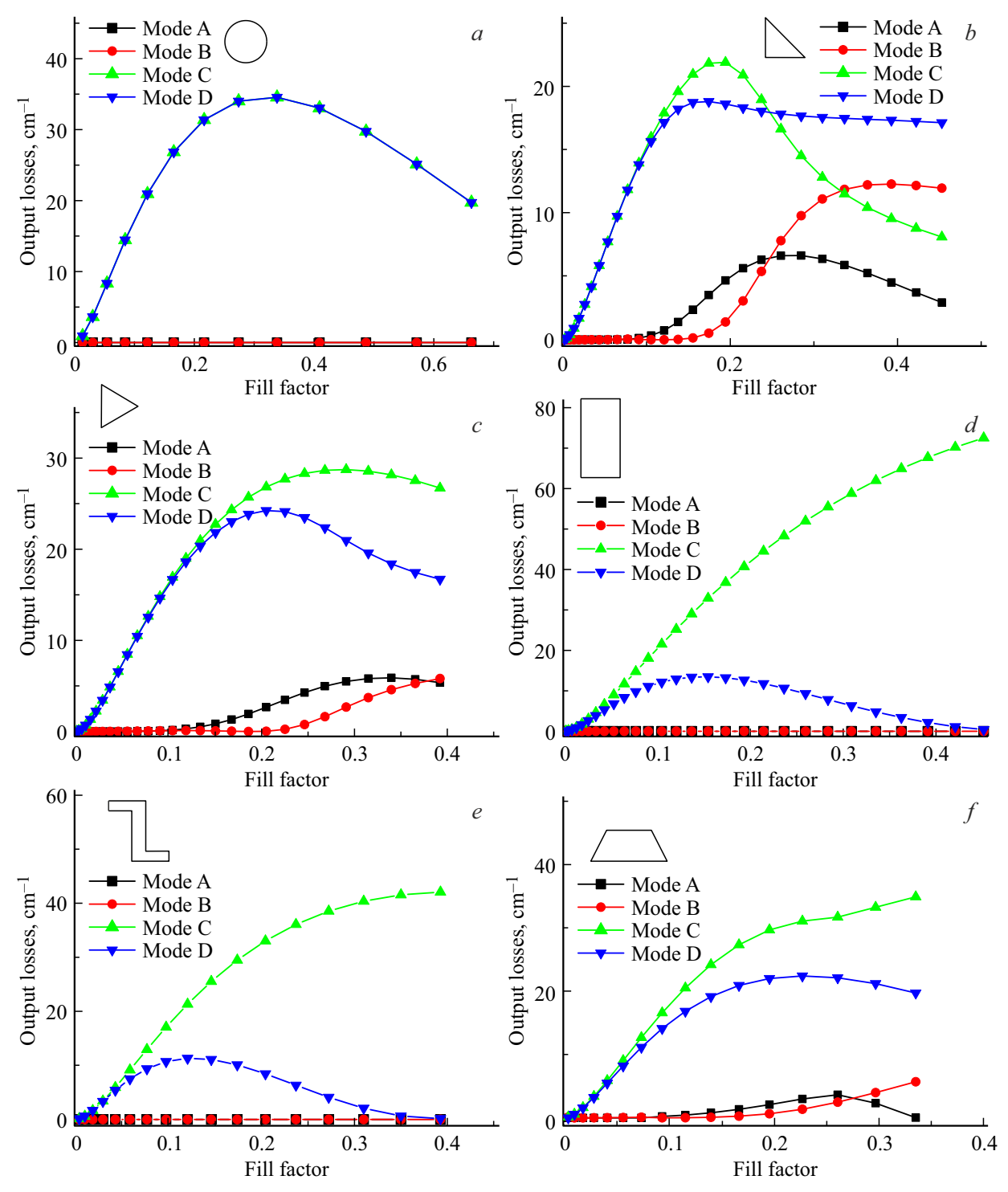


**Figure 3.** Output losses of a PC-based resonator with holes of various shapes at an etching depth of 1.9 microns, depending on the fill factor: a — circle, b — isosceles right triangle, c — equilateral triangle, d — rectangle, e —Z-shape, f — equilateral trapezoid.

holes that do not have a specular reflection, but have C<sub>2</sub>-symmetry. However, the presence of two zero-loss modes remains, which allows drawing a conclusion that it is the presence of C<sub>2</sub>-symmetry in the shape of the holes forming the PC that determines the presence of high-Q modes in the resonator.

Calculations were also performed for the trapezoidal shape of the holes (isosceles trapezoid, Figure 3, f), which demonstrated results similar to a right-angled triangle, which has the same symmetry group. Figure 4 shows patterns of the electric field strength (arrows) and its intensity (color) in the PC plane for trapezoidal holes with a fill factor of

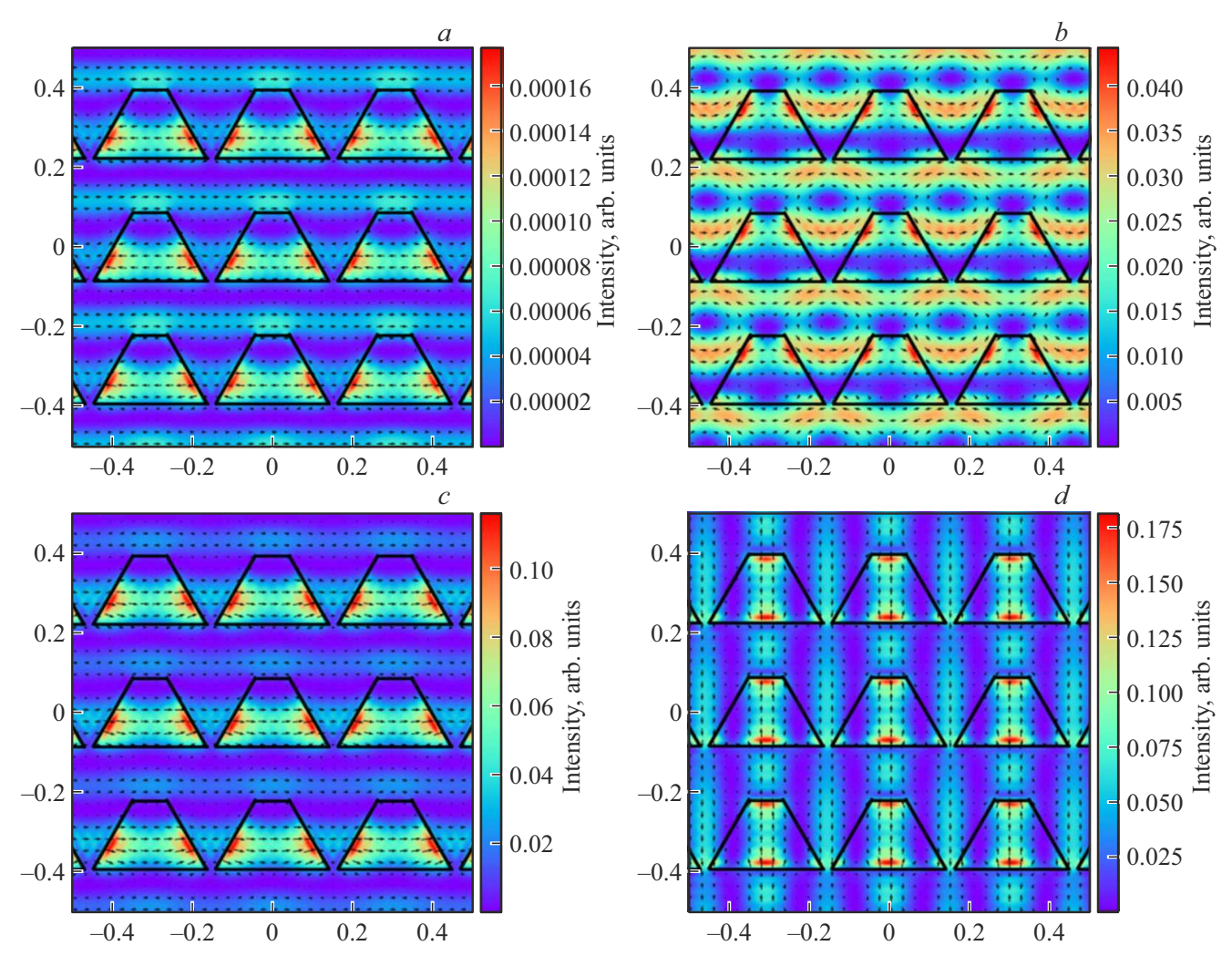


**Figure 4.** Distribution of electric field (arrows) and intensity (color) in PC with trapezoidal holes (solid black lines) with a fill factor of 33.5% for: a — mode A (output loss  $0.04 \,\mathrm{cm}^{-1}$ ), b — mode B ( $5.7 \,\mathrm{cm}^{-1}$ ), c — mode C ( $34.9 \,\mathrm{cm}^{-1}$ ), d — mode D ( $19.7 \,\mathrm{cm}^{-1}$ ).

33.5%, which is characterized by the fact that the output loss for mode A is almost zero. The spatial distribution of light intensity has a symmetry of PC lattice. The light intensity has the highest values in the area of air holes.

### 4.2. The effect of trapezoidal hole deformation on output losses

The variation of output losses during the transition from holes with symmetry  $C_2$ , which generate zero output losses to holes without symmetry  $C_2$ , was studied by calculating PC formed by an equilateral trapezoid, whose small base varies in size from zero to the magnitude of the large base. Thus, the geometry of the hole varied from an isosceles triangle to a rectangle with a symmetry of  $C_2$ . Figure 5 shows the results obtained for two modes — A and B, which have the lowest losses. The calculation was made for the dimensions of the large base and the height of the trapezoid, corresponding to the fill factor of 26% in Figure 3,f. However, the output losses decrease and

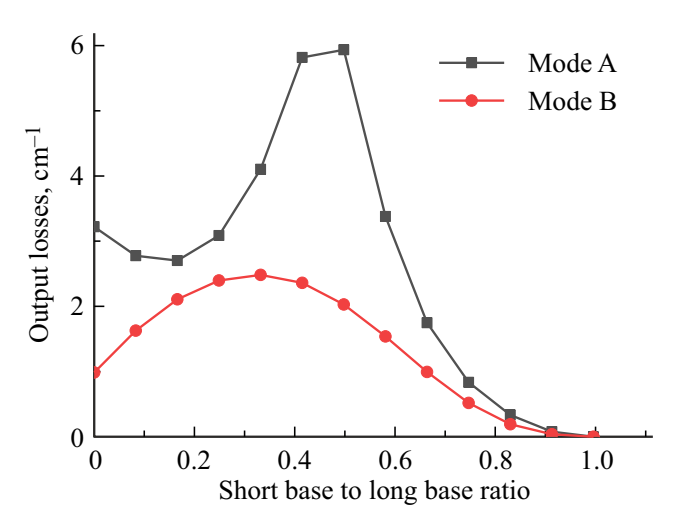


**Figure 5.** Output losses of a resonator based on PC with trapezoidal holes with an etching depth of 1.9 microns, depending on the ratio of the length of the small base to the length of the large base.

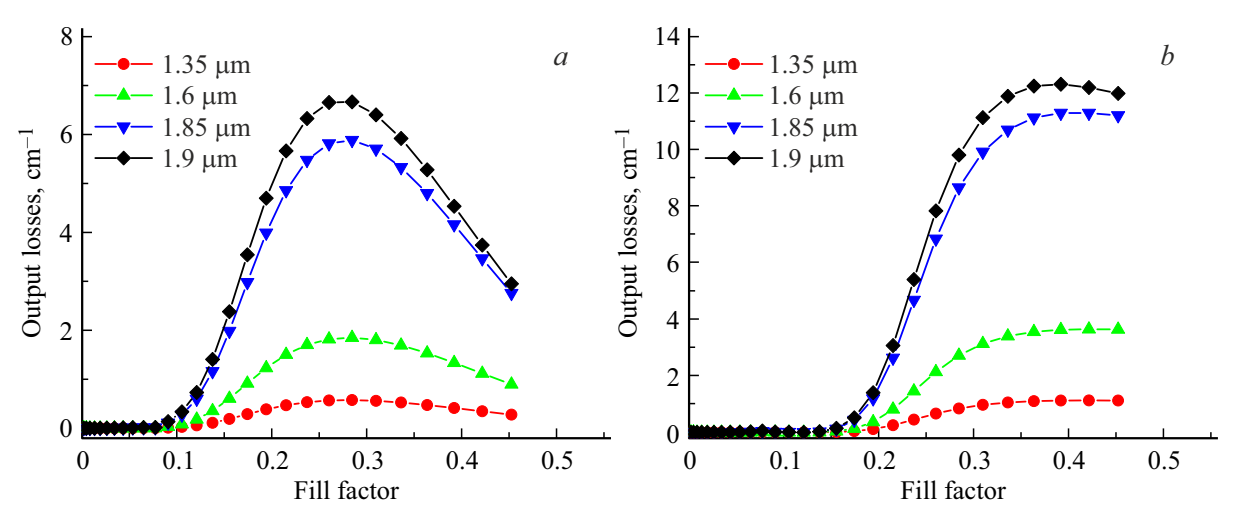


**Figure 6.** Dependence of the output loss on the etching depth of the air holes in the shape of an isosceles right triangle: a — mode A, b — mode B.

approach zero in case of transition from a trapezoid to a rectangle, as expected. The mode B is low-threshold over the entire range of the parameter. At the same time, modes A and B behave significantly differently. Mode A has a pronounced maximum at the values of the small base of the trapezoid  $\sim 50\%$  from the large one. Mode discrimination increases dramatically in this area, and the threshold conditions for mode A increase significantly, which makes this design the most suitable for single-mode generation.

#### Effect of the etching depth of air holes 4.3. on the outlet loss for holes of the isosceles right triangle type

We considered the dependence of the change in output losses on the etching depth of air holes for a surface 2D-PC, which provides a significant technological advantage due to the absence of two-stage epitaxial growth, with holes in the shape of an isosceles right triangle. The calculations were carried out at 3 different etching depths — 1.35, 1.6 and 1.85 microns. The results obtained were compared with the data on output losses for the initial etching depth — Since the A and B modes have minimal 1.9 microns. output losses, the loss dependences on the fill factor at different etching depths were analyzed specifically for them (Figure 6).

As can be seen in Figure 6, the nature of the dependencies does not change. The losses are simply scaled relative to the ordinate axis. At the highest etching depth (1.9 microns), maximum output losses are observed. This phenomenon is explained by the fact that with a decrease in the thickness of the residual layer (the emitter layer separating the PC region from the waveguide region), the optical restriction factor in the photonic crystal region increases, thus a large proportion of optical radiation from the waveguide penetrates into the PC region.

other hand, it could be expected that the PC layer, which has a lower dielectric constant, at greater etching depths will "squeeze out " the waveguide mode towards the *n*-emitter and, thus, reduce its own optical limitation factor. However, calculations of this particular PC design and the double heterostructure (DHS) have demonstrated that this effect does not occur at reasonable etching depths (there is no etching into the waveguide layer), which makes it possible to optimize the amount of resonator output losses by the etching depth parameter. The final optimization of the amount of output losses will be performed at a known amount of internal optical losses in a particular DHS. Thus, it can be concluded that etching of deep holes ( $\sim 1.8-1.9$  microns) with a very thin ( $\sim 0.1$  microns) residual layer between the crystal and the waveguide is the most effective, which should ensure the best coupling of the waveguide mode with the FC region.

### Conclusion

Calculations of optical output losses for a PC-based resonator formed by air holes of various geometric shapes in the AlGaAs/GaAs/InGaAs heterostructure demonstrated the relationship between hole symmetry and the dependence of loss values on the fill factor. 2D-PC with holes having symmetry C2 form a high-Q resonator unsuitable for the tasks of creating high-power injection semiconductor lasers. The calculation for a structure with holes in the form of an isosceles right triangle and an isosceles trapezoid demonstrated similar dependencies. At the same time, the trapezoid has another geometric parameter that can be independently changed, which allows you to control the mode discrimination between two low-threshold modes A and B. It is important to understand that as the geometric shape of the holes becomes more complex, the requirements for the technological processes of lithography and etching significantly increase. The calculation of the change of output losses depending on the etching depth shows that it is preferable to etch holes of great depth, leaving a thin  $(\sim 0.1\,\mathrm{microns})$  residual layer between the PC area and the waveguide, providing the most effective coupling of the waveguide mode with the PC. The design of the DHS affects both external and internal optical losses, which makes it possible to effectively optimize the value of the external differential quantum efficiency of the laser by adjusting the thickness of the waveguide and the depth of the holes.

### **Funding**

This study was supported financially by a grant from the Russian Science Foundation (project No. 23-72-01038).

### **Conflict of interest**

The authors declare that they have no conflict of interest.

### References

- M. Imada, S. Noda, A. Chutinan, T. Tokuda, M. Murata, G. Sasaki. Appl. Phys. Lett., 75 (3), 316 (1999).
   DOI: 10.1063/1.124361
- [2] M. Meier, A. Mekis, A. Dodabalapur, A. Timko, R.E. Slusher, J.D. Joannopoulos, O. Nalamasu. Appl. Phys. Lett., 74 (1), 7 (1999). DOI: 10.1063/1.123116
- [3] S. Noda, M. Yokoyama, M. Imada, A. Chutinan, M. Mochizuki. Science, 293 (5532), 1123 (2001). DOI: 10.1126/science.1061738
- [4] M. Imada, A. Chutinan, S. Noda, M. Mochizuki. Phys. Rev. B, 65 (19), 195306 (2002).
   DOI: 10.1103/PhysRevB.65.195306
- [5] I. Vurgaftman, J.R. Meyer. IEEE J. Quant. Electron., 39 (6), 689 (2003). DOI: 10.1109/JQE.2003.811943
- [6] D. Ohnishi, T. Okano, M. Imada, S. Noda. Opt. Express, 12 (8), 1562 (2004). DOI: 10.1364/opex.12.001562
- [7] M. Yoshida, M. Kawasaki, M. De Zoysa, K. Ishizaki, T. Inoue,
   Y. Tanaka, R. Hatsuda, S. Noda. Proc. IEEE, 108 (5), 819 (2020). DOI: 10.1109/JPROC.2019.2935159
- [8] M. Yoshida, M. De Zoysa, K. Ishizaki, Y. Tanaka, M. Kawasaki, R. Hatsuda, B. Song, J. Gelleta, S. Noda. Nature Materials, 18 (2), 121 (2019). DOI: 10.1038/s41563-018-0242-v
- [9] K. Kitamura, M. Kitazawa, S. Noda. Opt. Express, 27 (2), 1045 (2019). DOI: 10.1364/oe.27.001045
- [10] R. Sakata, K. Ishizaki, M. De Zoysa, S. Fukuhara, T. Inoue, Y. Tanaka, K. Iwata, R. Hatsuda, M. Yoshida, J. Gelleta, S. Noda. Nature Commun., 11 (1), 1 (2020). DOI: 10.1038/s41467-020-17092-w
- [11] E. Miyai, K. Sakai, T. Okano, W. Kunishi, D. Ohnishi, S. Noda. Nature, 441 (7096), 946 (2006). DOI: 10.1038/441946a
- [12] M. Yokoyama, S. Noda. IEICE Trans. Electron., 87 (3), 386 (2004).
- [13] M. Yokoyama, S. Noda. Opt. Express, 13 (8), 2869 (2005). DOI: 10.1364/OPEX.13.002869
- [14] D.-U. Kim, S. Kim, J. Lee, S.-R. Jeon, H. Jeon. IEEE Photon. Technol. Lett., 23 (20), 1454 (2011). DOI: 10.1109/LPT.2011.2162944

- [15] L.-R. Chen, K.-B. Hong, K.-C. Huang, H.-T. Yen, T.-C. Lu. Opt. Express, 29 (7), 11293 (2021). DOI: 10.1364/OE.421019
- [16] K.-B. Hong, L.-R. Chen, K.-C. Huang, H.-T. Yen, W.-C. Weng, B.-H. Chuang, T.-C. Lu. IEEE J. Select. Top. Quant. Electron., 28 (1), 1 (2022). DOI: 10.1109/JSTQE.2021.3095961
- [17] S. Saito, R. Hashimoto, K. Kaneko, T. Kakuno, Y. Yao, N. Ikeda, Y. Sugimoto, T. Mano, T. Kuroda, H. Tanimura, S. Takagi, K. Sakoda. Appl. Phys. Express, 14 (10), 102003 (2021). DOI: 10.35848/1882-0786/ac2240
- [18] H. Kogelnik, C.V. Shank. J. Appl. Phys., 43 (5), 2327 (1972). DOI: 10.1063/1.1661499
- [19] W. Streifer, D. Scifres, R. Burnham. IEEE J. Quant. Electron.,
   13 (4), 134 (1977).
   DOI: 10.1109/JQE.1977.1069328
- [20] K. Sakai, E. Miyai, S. Noda. Appl. Phys. Lett., 89 (2), 021101 (2006). DOI: 10.1063/1.2220057
- [21] K. Sakai, E. Miyai, S. Noda. IEEE J. Quant. Electron., 46 (5), 788 (2010). DOI: 10.1109/JQE.2009.2037597
- Y. Liang, C. Peng, K. Sakai, S. Iwahashi, S. Noda. Phys. Rev. B, 84 (19), 195119 (2011).
   DOI: 10.1103/PhysRevB.84.195119
- [23] K. Sakai, E. Miyai, T. Sakaguchi, D. Ohnishi, T. Okano, S. Noda. IEEE J. Select. Areas Commun., 23 (7), 1335 (2005). DOI: 10.1109/JSAC.2005.851205
- [24] M. Plihal, A. Shambrook, A. A. Maradudin, P. Sheng. Optics Commun., 80 (3-4), 199 (1991).
   DOI: 10.1016/0030-4018(91)90250-H
- [25] F. Bloch. Zeitschrift Physik, 52 (7), 555 (1929).DOI: 10.1007/BF01339455
- [26] S. Adachi. J. Appl. Phys., 58 (3), R1 (1985).DOI: 10.1063/1.336070

Translated by A.Akhtyamov